Friction **9**(5): 978–989 (2021)
https://doi.org/10.1007/s40544-020-0383-2
ISSN 2223-7690
CN 10-1237/TH
RESEARCH ARTICLE

A synergetic strategy based on laser surface texturing and lubricating grease for improving the tribological and electrical properties of Ag coating under current-carrying friction

Zhengfeng CAO[1,*], Yanqiu XIA[2,*], Chuan CHEN[2,3], Kai ZHENG[1], Yi ZHANG[1]

[1] *School of Advanced Manufacturing Engineering, Chongqing University of Posts and Telecommunications, Chongqing 400065, China*

[2] *School of Energy Power and Mechanical Engineering, North China Electric Power University, Beijing 102206, China*

[3] *Global Energy Interconnection Research Institute Co., Ltd., Beijing 102211, China*

Received: 19 September 2019 / Revised: 17 February 2020 / Accepted: 15 March 2020

Abstract: Herein, a series of Ag coatings with different micro-dimples were fabricated on copper surfaces by laser surface texturing (LST) and magnetron sputtering. Multilayer graphene lubricating grease (MGLG) was prepared using multilayer graphene as an additive. The textured Ag coatings and MGLG were characterized. Moreover, the tribological and electrical performances of the textured Ag coatings under MGLG lubrication were investigated in detail. Results demonstrated that the textured Ag coating with an appropriate dimple diameter could exhibit improved tribological and electrical properties when compared to the non-textured Ag coating under MGLG lubrication. The characterization and analysis of the worn surfaces suggest that the synergetic effect of LST and MGLG contributes to these excellent tribological and electrical properties.

Keywords: laser surface texturing; tribology; contact resistance; lubricating grease

1 Introduction

Sliding electrical connectors have attracted considerable attention in academic and industrial fields due to their involvement in extremely complex phenomena including mechanical, electrical, thermal, and material aspects [1–4]. To achieve a high level of reliability and service life, sliding electrical materials should possess a combination of characteristics, which include superior friction reduction, anti-wear abilities, low electrical contact resistance (ECR), and preferable corrosion resistance. At present, sliding electrical contacts are usually coated with soft noble metals such as Ag and Au, which can provide a relatively large real contact area, an excellent conductivity, and preferential corrosion and oxidation resistances [4–6]. However, the tribological performance, which greatly impacts the reliability and service life of sliding electrical connectors, is currently unsatisfactory [4, 5].

Wear is one of the major factors leading to the deterioration and failure of sliding electrical connectors and the wear mechanisms are mainly attributed to abrasive and adhesive wear [7, 8]. The operating temperature of sliding electrical connectors usually fluctuates over a wide range due to friction, wear, electrical current, and arc erosions [9]. Trinh et al. reported that the maximum temperature may achieve ~150 °C [8]. At high temperatures, the soft noble coating is more susceptible to peeling, thereby producing wear debris and forming an adhesion region. Some wear debris may function as abrasive particles, thus damaging the surface coatings and resulting in an increased wear and ECR in the process of friction. Some wear debris may soften, then deposit on the rubbing surfaces to form a transfer layer [7]. Although this transfer layer may improve the tribological

* Corresponding authors: Zhengfeng CAO, E-mail: caozf@cqupt.edu.cn; Yanqiu XIA, E-mail: xiayq@ncepu.edu.cn

properties, it will undoubtedly increase the ECR. Therefore, it is of utmost significance to reduce the formation of wear debris to improve the quality of sliding electrical connectors.

Laser surface texturing (LST), an artificial topography created on the contact surface, is a well-known approach to improve the tribological properties [10–13]. An important lubrication mechanism of LST is the effective micro-dimples, which can store the wear debris, thereby reducing the surface damage [11–13]. This advantage of LST could be utilized to reduce the negative impact of sliding electrical contacts caused by wear debris. However, Huang et al. postulated that the lifetime and service performances of the electrical connectors were significantly impacted by the stability of friction and ECR [14]. From another perspective, LST increases the surface roughness, which may cause a large fluctuation in tribological and conductive behaviors.

Lubricants could be further employed to address the limitations caused by LST. These lubricants have numerous remarkable characteristics such as minimizing wear, cooling, sealing, and corrosion inhibition [15, 16]. When the surface texture associates with the lubricant, the combination can exhibit some synergistic lubrication mechanisms including acting as micro-reservoirs of lubricants to increase the local lubricant supply and functioning as micro-hydrodynamic bearings to increase the load-carrying capacity, which can greatly enhance the tribological properties [8, 17–19]. However, the lubricant applied for sliding electrical contacts should possess outstanding lubricating ability and preferable conductivity [20–22]. When performing the functions of friction reduction, anti-wear, cooling, and corrosion prevention, the lubricants could also form conductive paths to transmit current between the contact interfaces, thereby reducing the ECR.

In this work, a synergetic strategy based on LST and conductive lubricants was proposed to improve the tribological and electrical performances of Ag coating for sliding electrical connectors. A series of surface textures with different sizes were created on copper disc surfaces using a laser system. Then, Ag coatings were deposited on the textured surfaces by a magnetron sputtering system. The conductive lubricating grease was prepared using bentone grease as the base grease and graphene as the additive due to the preferable colloidal stability and environmentally friendliness of bentone grease and the excellent tribological properties, high conductivity, and novel thermal capacity of graphene [23–25]. The tribological and electrical performances of the Ag-coated textured copper discs that were lubricated using graphene lubricating grease were investigated in detail. Meanwhile, according to our previous work [26], the stability of friction and ECR were quantitatively assessed by standard deviation. Moreover, the mechanisms of the tribological and electrical performances were analyzed based on the characterization of the rubbing surfaces.

2 Experimental procedures

2.1 Materials

The base oil of polyalkylene glycol (PAG) was commercially available from Dow Chemical Co., Ltd.; Table 1 outlines the typical characteristics. Bentonite and acetone (analytical grade) were commercially obtained from Sinopharm Chemical Reagent Co., Ltd. The multilayer graphene (MG) was obtained from State Key Laboratory of Solid Lubrication, Chinese Academy of Sciences (Lanzhou, China).

2.2 Laser surface texturing of the copper substrates

The copper was cut into a 25 mm × 25 mm disc to form the substrate. The surface roughness was ~0.05 μm after polishing process. Next, micro-scale dimples were fabricated on the copper surfaces using a pulsed neodymium-doped yttrium aluminum garnet laser (Nd:YAG, CLS8100, Lase-Sino Technology Co., Ltd.) with a wavelength of 1,064 nm. The frequency and the average power were set at 8 kHz and 50 W, respectively.

Table 1 Typical properties of PAG.

Item	Kinematic viscosity (mm^2/s)		Viscosity index	Pour point (°C)	Fire point (°C)	Volume resistivity (μΩ·cm)
	40 °C	100 °C				
PAG	320	36	163	–37	260	3.2×10^5

2.3 Deposition and characterization of Ag coating

After LST, the samples were ultrasonically cleaned in acetone for 10 min. Subsequently, fine Ag coatings were fabricated by magnetron sputtering from high-purity Ag targets (>99.9%). The base pressure at the initial deposition process was ~6×10^{-3} Pa. The substrate bias and DC power supply were 200 V and 500 W, respectively. The process pressure during deposition was ~0.3 Pa under Ar flow.

The hardness and elastic modulus were determined using a Hysitron triboindenter (TI 980, Bruker). The LST, depth, and cross section of the dimples were characterized using scanning electron microscopy (SEM, EVO-18, Zeiss) and energy-dispersive X-ray spectroscopy (EDX, Bruker). The phase analysis of the Ag coating was conducted using X-ray diffraction (XRD, Bruker, Germany) with a copper tube (Kα, λ = 1.54 Å).

2.4 Preparation and characterization of lubricating grease

The lubricating grease was synthesized using the following procedure. First, the PAG (85 wt%) and the MG (0.2 wt%) were placed in the reaction vessel and subsequently agitated. Second, the bentonite (15 wt%) and acetone (5 mL) were successively added to the reaction vessel and consistently stirred (~30 min). Then, the mixture was heated to 80 °C for another 30 min to remove the acetone. Finally, the mixture was cooled to 25 °C, then grinded and homogenized by a three-roller mill to produce the multilayer graphene lubricating grease (labeled MGLG).

The physical properties including penetration, corrosion, and dropping point were characterized according to the national standards GB/T 269, GB/T 7326, and GB/T 3498, which are equivalent to ASTM D2265, ASTM 130-83, and ASTM D1404, respectively. A GEST-121 surface volume resistivity was used to characterize the conductivity. A thermogravimetric analyzer (TGA, Q500, TA Instruments) was employed to conduct the thermal analysis of MG and MGLG under a flow of air. The heating rate was set at 10 °C /min.

2.5 Tribological test under applied current

An MFT-R4000 reciprocal tribometer was utilized to assess the tribological and electrical performances of the samples under current-carrying conditions. Figure 1 depicts a schematic of the apparatus used in the current-carrying friction test. A stable voltage could be provided by the power supply and the contact current was recorded in real time. The friction pair comprised of a copper ball (diameter: 5 mm, hardness: 120 HV) and the lower as-prepared Ag-coated textured disc (25 mm × 25 mm). The copper ball slid reciprocally against the lower disc under low (5 A) and high (50 A) current. The amplitude, frequency, and applied load were set at 5 mm, 2 Hz, and 5 N, respectively. The corresponding current densities of the low and high currents were approximately 0.47 and 4.7 GA/m^2, respectively. During the friction process, a computer automatically recorded the curves of applied voltage and coefficients of friction (COF) as a function of time.

After tribological testing, the ECR was calculated by Ohm's law. The mean values ($\bar{x}$) and stand deviations (SD) were calculated by Eqs. (1) and (2), respectively, and used to assess the stability of the COF and ECR.

$$\bar{x} = \frac{1}{n}\sum_{i=1}^{n} x_i \tag{1}$$

$$\mathrm{SD} = \sqrt{\frac{1}{n}\sum_{i=1}^{n}(x_i - \bar{x})^2} \tag{2}$$

where x_i and n represent the instantaneous value and the number of the instantaneous values, respectively.

2.6 Characterization of the worn surfaces

After tribological testing, the lower disks were cleaned

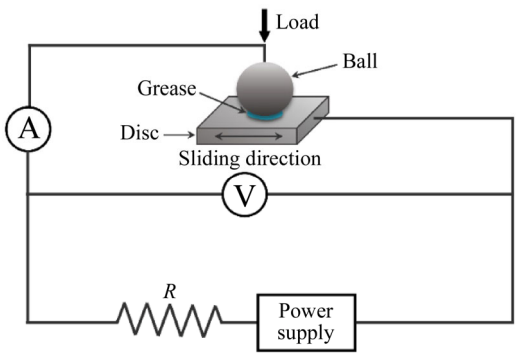

Fig. 1 Schematic representation of the apparatus used in the current-carrying friction test.

by an ultrasonic cleaner comprised of acetone. Then, an optical microscope (Olympus, Japan) was employed to acquire the wear widths. SEM and EDX were utilized to obtain the surface topographies and chemical compositions of the rubbing surfaces, respectively. X-ray photoelectron spectroscopy (XPS, PHI-5702) was utilized to conduct analyses on the chemical states of the typical elements in the rubbing surfaces. A carbon binding energy of 284.6 eV was used as the reference and the pass energy was 29.3 eV with a resolution of approximately ±0.3 eV.

3 Results and discussion

3.1 Analysis of the Ag coating

The crystalline structure of the Ag coating was identified using XRD, as shown in Fig. 2(a). The as-deposited coating exhibits the characteristics peaks of the (111), (200), (220), and (311) planes corresponding to the Ag–3C diffraction peaks, thus indicating that the Ag coating has a face-centered cubic crystal structure [27]. The XRD result confirms that the as-deposited Ag coating is highly purified, without a crystalline or heterogeneous phase. Figure 2(b) depicts the cross-sectional SEM image with an EDX line scan of the Ag coating, which could determine that the thickness of the Ag coating is ~22.7 μm. By observing the image, we postulated that the transition region was natural and the Ag coating had been tightly integrated with the Cu substrate, demonstrating a good adhesion. In contrast, the mechanical tests reveal that all the coatings were fabricated by the same preparation process. Therefore, the hardness values and elastic moduli are close, ranging from ~103–108 HV and ~76–79 GPa, respectively.

Figure 3 reveals the SEM images of the Ag-coated textured surfaces with the cross-sectional images of

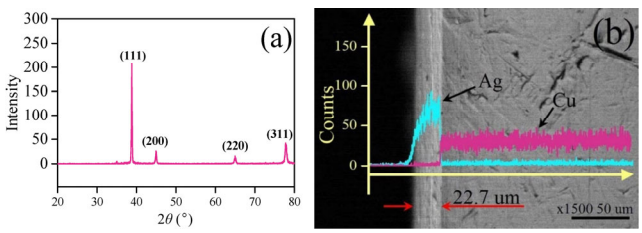

Fig. 2 (a) XRD pattern and (b) cross-sectional SEM image with EDX line scan of the Ag coating.

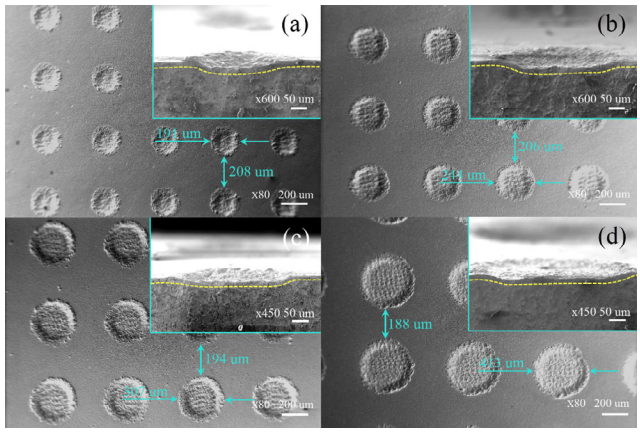

Fig. 3 SEM images of the textured surfaces and the cross-sectional images of the dimples: (a) T1, (b) T2, (c) T3, and (d) T4.

the dimples. By observing the images, we determined that the diameters of the dimples were approximately 191, 244, 307, and 413 μm after deposition of the Ag coating; the corresponding dimple densities were approximately 19%, 24%, 28%, and 35%, respectively. All the dimples exhibited similar depths; in particular, the depths of T1, T2, T3, and T4 were 42.7, 43.3, 43.2, and 43.5 μm, respectively. Herein, the non-textured Ag coating and the textured Ag coatings were labeled as Ag, T1, T2, T3, and T4, respectively.

3.2 Analysis of MG and MGLG

Figure 4(a) depicts the SEM image of MG. MG exhibits a large two-dimensional planar structure, which is beneficial for promoting contact between the graphene sheets in grease to form a network, which improves the electrical and thermal conductivities of the grease. Moreover, this network functions as a protective film to minimize the friction and wear [20, 25]. Figure 4(b) depicts the thermal stability of MG and MGLG. MG begins to decompose at ~220 °C, which is attributed to the removal of the pyrolysis

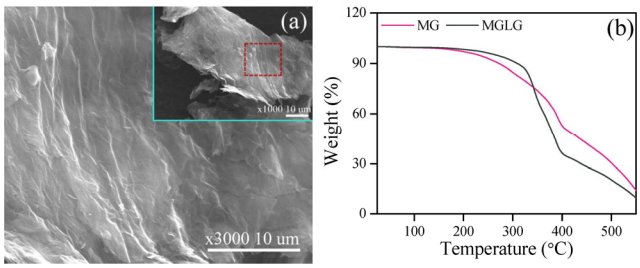

Fig. 4 (a) SEM image of the MG and (b) TGA curves of MG and MGLG

of the carbon skeleton and labile oxygen-containing functional groups. MGLG has a higher decomposition (~250 °C) than MG, which may be due to the relatively low MG content in grease. Therefore, the thermal stability of MGLG is mainly dependent on the base grease. Table 2 outlines the physical characteristics of the base grease and MGLG. The results show that MGLG has a lower penetration and higher dropping point than the base grease, which may be attributed to the high special surface area of MG that could prevent liquid molecules from moving [20]. The addition of MG reduced the volume resistivity of the base grease by up to ten times, which indicates that MGLG exhibits better conductivity than the base grease. The TGA analysis and physical properties demonstrate that MGLG has preferential thermal stability and anti-corrosion performance, which could fulfil the requirements of sliding electrical contacts.

3.3 Tribological and electrical properties under low current density

Figure 5 yields the COF, ECR, SD values, and wear width of the samples under a low current density of 0.47 GA/m^2. As shown in Fig. 5(a), the Ag coating under dry friction exhibited a very high COF (up to ~0.789). In contrast, when MGLG was employed, the COFs of the non-textured and textured samples were significantly lower. Therein, T2 achieved the lowest COF (~0.101), indicating that MGLG could greatly improve the tribological properties. Figure 5(b) exhibits the ECR curves of different samples during the friction process. It is visible that all the samples exhibited similar ECR values at the beginning of the friction. As friction continued, the ECR of the Ag coating under dry friction gradually increased, whereas that of the other specimens gradually decreased. Therein, the T2 lubricated by MGLG exhibited the lowest ECR after the running-in period. Figure 5(c) yields the SD values of COF and ECR. The Ag coating under dry friction

Table 2 Physical characteristics of the base grease and MGLG.

Sample	Penetration (mm)	Dropping point (°C)	Copper corrosion (T2 copper, 100 °C, 24 h)	Volume resistivity (μΩ·cm)
Base grease	398	273	1a	2.7×10^5
MGLG	375	293	1a	3.8×10^4

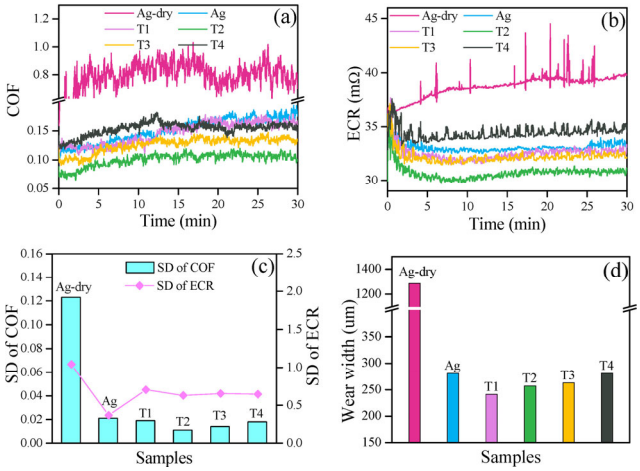

Fig. 5 (a) COF, (b) ECR, (c) SD values, and (d) wear width of the samples under a low current density of 0.47 GA/m^2.

exhibits considerably larger SD values than the other specimens. The MGLG lubricated T2 exhibited the lowest SD value of COF, indicating the combination of LST and MGLG contributed to a much lower and stable tribological behavior. All the textured Ag coatings exhibited higher SD values of ECR than non-textured Ag coatings, which may be due to the surface texture. Although the surface texture was filled with MGLG and wear debris, the conductivity was lower than that of Ag. When the upper ball traveled across the dimples, ECR exhibited a little large fluctuation. Figure 5(d) shows that the anti-wear ability was greatly enhanced by the MGLG because the wear width of Ag under dry friction was significantly larger than that of other specimens. The wear widths of T1 and T2 are slightly smaller than that of Ag under MGLG lubrication, indicating that the synergetic strategy of MGLG and LST could also exhibit a better anti-wear ability.

Figure 6 depicts the SEM images of the worn surfaces under a low current density of 0.47 GA/m^2. The Ag coating under dry friction exhibited a considerably wide wear scar (~1,285 μm) and numerous grooves and spalling appeared on the rubbing surfaces, thus indicating a harsh lubrication condition. When the MGLG was applied, all the wear widths of the samples were greatly reduced, indicating an excellent anti-wear ability. The area of all the different dimples became smaller after friction test. (The red circles highlight the dimple sizes before the friction test). The reason for this may be attributed to the fact that

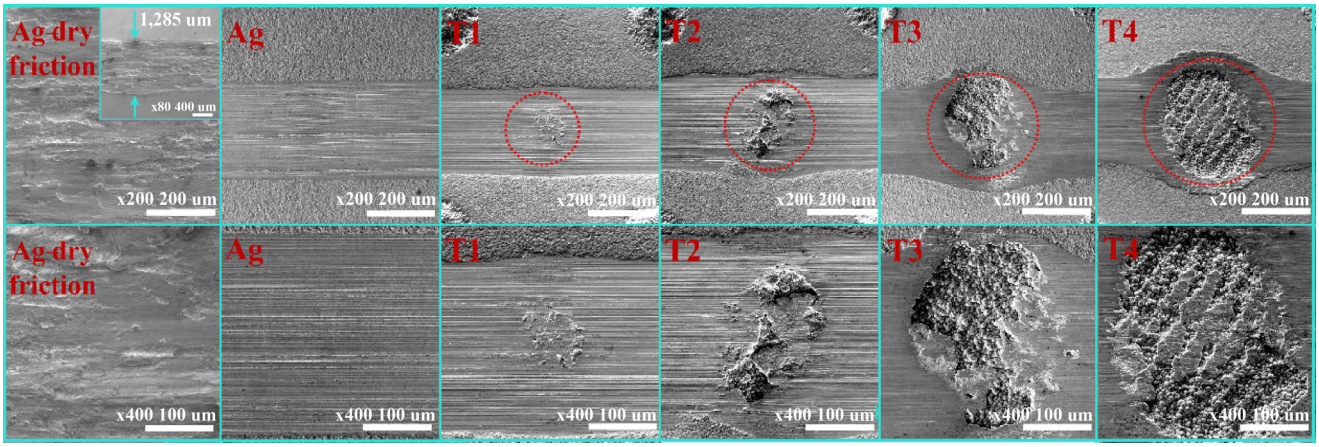

Fig. 6 SEM images of the worn surfaces on the samples after the friction test under a low current density of 0.47 GA/m^2.

Ag exhibits good malleability; moreover, the wear debris of Ag could soften and deposit in the dimples during the friction process. In particular, the dimple with a relatively small diameter in T1 disappeared after friction testing. Based on the results shown in Fig. 5, T1 exhibited a relatively high COF and ECR, which may be due to the disappearance of the dimple, resulting in the failure of the synergistic effect based on LST and MGLG. This result also explains why the reason for the enhanced electrical and tribological performances of T2 was ascribed to the synergistic effect based on LST and MGLG. In terms of T3 and T4, due to relatively large diameters of the dimples, their electrical and tribological properties were not adequately favorable. A suitable dimensional design of the dimples has significant influence on the tribological and electrical properties.

3.4 Tribological and electrical properties under a high current density

Figure 7 depicts the COF, ECR, SD values, and wear width of the samples under a high current density of 4.7 GA/m^2. As shown in Fig. 7(a), when the current density increased to 4.7 GA/m^2, severe wear occurred on the Ag coating under dry friction because it exhibited a tremendous increase in the COF and noise. The MGLG significantly reduced the COF; the lowest COF (~0.162) was obtained by T3, indicating that MGLG and LST achieved an excellent synergistic effect to improve the tribological properties. The ECR curves shown in Fig. 7(b) suggest that the electrical performances following the improvement of tribological properties were also significantly enhanced, which was also attributed to the synergistic effect of MGLG and LST. Figure 7(c) shows the corresponding SD values. T4 possessed the highest SD values of COF and ECR, which may be due to the relatively large dimple diameter. Ag and T3 exhibited similar SD values of COF and ECR. Figure 7(d) depicts the wear width of the samples under high current density. T3 had the lowest wear width of all the coatings, which indicates that the combination of MGLG and LST with an appropriate size could exhibit superior friction reduction, anti-wear, and electrical behaviors.

Figure 8 depicts the SEM images of the worn surfaces under a high current density of 4.7 GA/m^2. The Ag coating revealed several shallow furrows and adhesion regions that may be dominated by abrasive and adhesive wear. The area of the dimples reduced

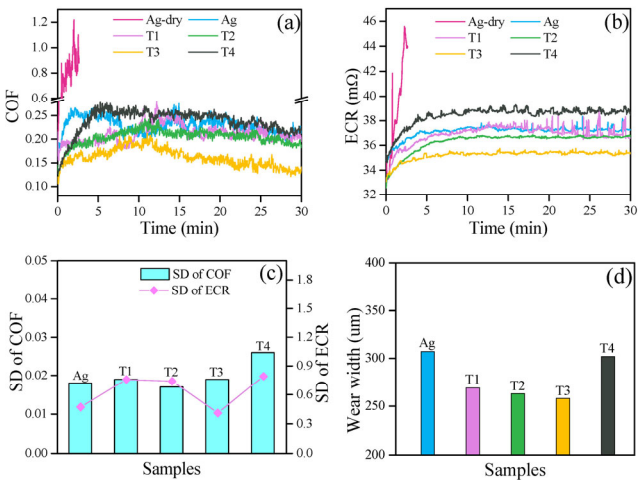

Fig. 7 (a) COF, (b) ECR, (c) SD values, and (d) wear width of the samples under a high current density of 4.7 GA/m^2.

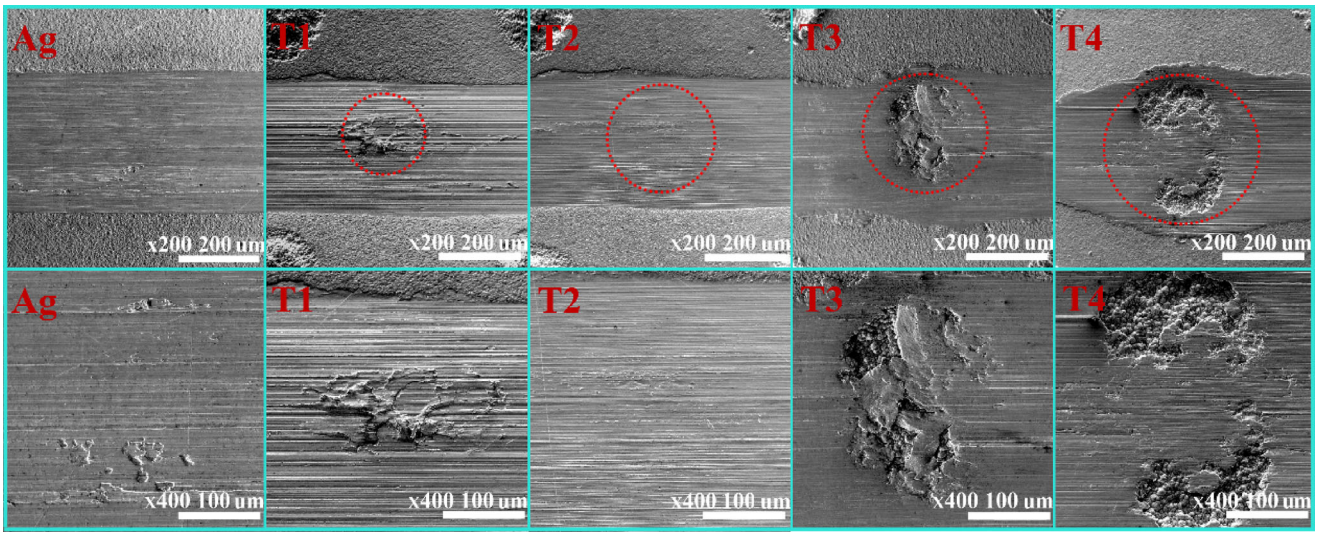

Fig. 8 SEM images of the worn surfaces on the samples after friction test under a high current density of 4.7 GA/m^2.

further after friction testing compared with that of the worn surfaces shown in Fig. 6, which may be due to the high current density, which results in more wear debris and coating softening. The dimple remained on the rubbing surface of T3 and was filled with wear debris after friction testing, thus indicating that the synergistic effect of LST and MGLG was ever-present to enhance the tribological and electrical performances in the process of friction.

3.5 Tribological and electrical properties of heat-treated samples

In general, intermittent high temperature may be generated in the electrical contact zone due to the variable current, which may greatly impact the tribological and electrical performances of the sliding electrical contacts [9]. Given that the coating and the substrate usually have different thermal expansion coefficients, the binding force between the two will be greatly impacted when subjected to heat treatment. Therefore, it is necessary to investigate the tribological and electrical performances of the heat-treated samples. Trinh [8] reported that the highest temperature of electrical contacts may reach ~150 °C; therefore, the samples were heated for 24 h at a temperature of 150 °C. Then, they were cooled to room temperature and their tribological and electrical properties were investigated under a high current density.

Figures 9(a) and 9(b) show the evolution of COF and ECR for the heat-treated samples as a function of time. The Ag coating exhibited a higher COF and ECR under both dry friction and MGLG lubrication. T3 exhibited the lowest COF and ECR throughout the friction process. Moreover, the COF and ECR of the heat-treated samples were higher than those of the non-treated samples shown in Figs. 7(a) and 7(b), indicating that heat treatment had a negative influence on the tribological and electrical properties. Figure 9(c) suggests that all the samples possessed similar SD values of ECR, whereas T3 revealed the lowest SD values of COF, indicating that T3 exhibited a more stable tribological behavior during the friction process. T2 and T3 exhibit similar wear widths, with values

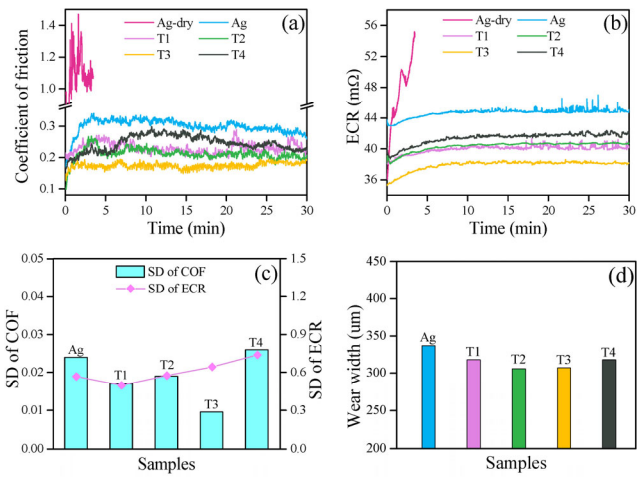

Fig. 9 (a) COF, (b) ECR, (c) SD values, and (d) wear width of the heat-treated samples under a high current density of 4.7 GA/m^2.

lower than that for the Ag coating (Fig. 9(d)). These results demonstrate that under MGLG lubrication, the dimple with an appropriate size could make a positive contribution to the anti-wear ability of the coating.

Figure 10 depicts the SEM images of the rubbing surfaces for the heat-treated samples after friction testing under a high current density of 4.7 GA/m^2 and is similar to the results shown in Fig. 8. The area of dimples significantly reduced and the dimples remained on the worn surfaces of T3 and T4, indicating that the dimples and MGLG always exhibited the synergistic effect, which improved the tribological and electrical properties during the friction process.

3.6 Function of MG in the lubricating grease

The tribological and electrical performances of Ag, T2, and T3 under different current densities and in the presence or absence of MG were investigated to demonstrate the function of the multilayer graphene in the lubricating grease (Fig. 11). A comparison of the experimental results under base grease and MGLG lubrication revealed that all the COFs, ECRs, and wear widths under MGLG lubrication were smaller than those under base grease lubrication, which demonstrated that MG played a significant function during the friction process, as shown in Figs. 11(a)–11(c). MG effectively formed tribological and conductive films on the worn surface to enhance the friction-reducing, anti-wear, and electrical performances. In addition, the coatings under high current density exhibited higher COFs, ECRs, and wear widths than those under low current density, regardless of whether MG was present. The aforementioned trend may be due to the fact that the high current density could generate more heat in the friction zone, which may contradict the formation of lubricating and conductive films.

3.7 Extreme pressure performances of the samples

To further investigate the influence of LST on the

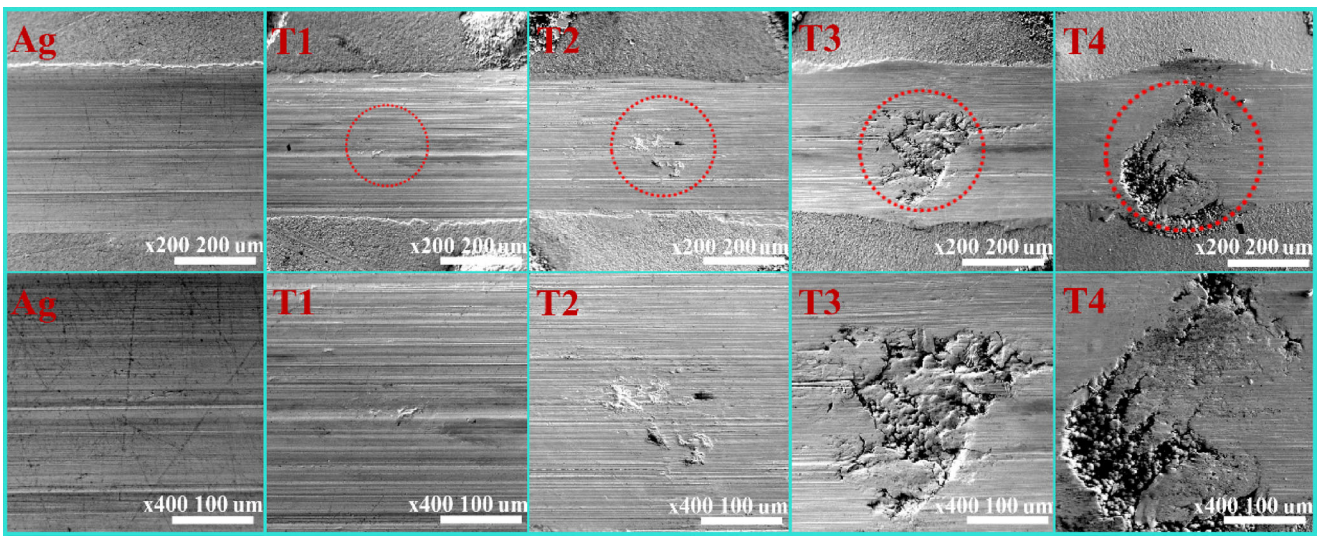

Fig. 10 SEM images of the rubbing surfaces of the heat-treated samples after friction test under a high current density of 4.7 GA/m^2.

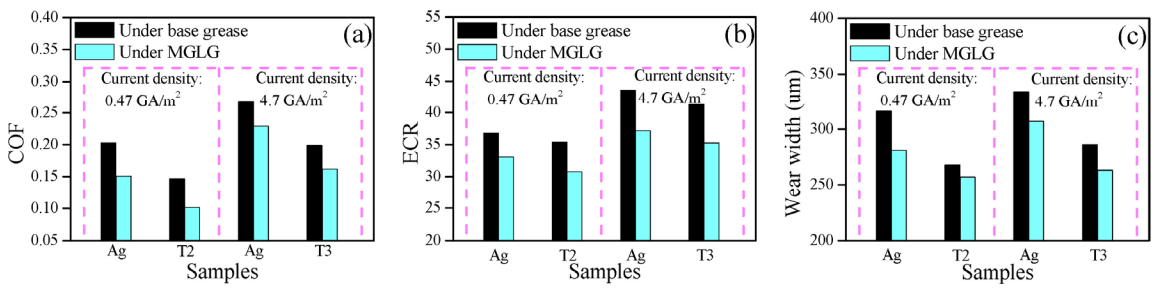

Fig. 11 (a) COF, (b) ECR, and (c) wear width of Ag, T2, and T3 under different current density and in the presence and absence of MG.

coatings, the extreme pressure performances of the samples (Ag and T3) and heat-treated samples (treated Ag and treated T3) under dry friction were conducted (Fig. 12(a)). All the samples exhibited similar evolutions of COF that they were relatively low at the initial stage, then increased sharply. T3 exhibited a lower COF than Ag, which was due to the fact that the dimples on T3 could effectively capture the wear debris. However, the extreme pressure performance of T3 was lower than that of Ag because stress concentration was easily generated around the dimple edges [11].

All the heat-treated samples exhibited higher COFs and lower extreme pressure performances than the corresponding non-heat-treated samples, which may be due to the fact that heat treatment reduced the binding force between the substrate and the coatings. However, the heat-treated T3 exhibited a lower COF and higher extreme pressure performance than the heat-treated Ag because the dimples could effectively capture the wear debris and prevent the decrease in the binding force caused by heat treatment. Figure 12(b) gives a schematic of thermal stress concentration on the heat-treated samples. As mentioned above, due to the various thermal expansion coefficients between the coating and the substrate, thermal stress concentrations could occur in the coatings when subjected to heat treatment (Fig. 12(b)), thereby resulting in a decreased binding force and peeling of the coating. However, when LST was performed on the coating, these dimples could promote concentration of the thermal stress around the edges of the dimples. This stress concentration may be dissipated as shown in Fig. 12(b), thereby preventing a decrease in the binding force between the coating and the substrate, which may be attributed to the better extreme pressure performance of the heat-treated T3 than that of the heat-treated Ag.

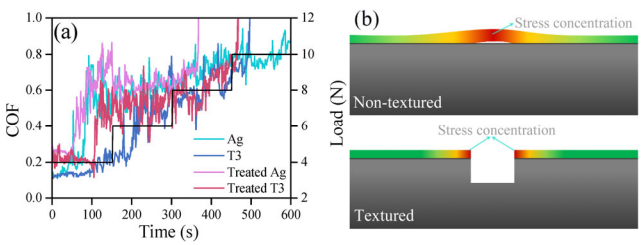

Fig. 12 (a) Extreme pressure performances of the samples and heat-treated samples under dry friction. (b) Schematic of thermal stress concentration on the heat-treated samples.

3.8 EDX and XPS analysis of the worn surfaces

Figure 13 depicts the EDX and XPS curves of the characteristic elements on the worn surfaces after the friction test. As shown in Fig. 13(a), the Cu appearing on the Ag coating under dry friction indicates that there was severe wear contributing to the high COF and ECR, which was consistent with the results shown in Figs. 5 and 6. Figure 13(b) reveals that a large quantity of C was detected on the outside of the dimple, indicating that MG was present on the worn surface to form a lubricating film to enhance the tribological and electrical performances. Figure 13(c) suggests that the dimples on the textured worn surface could function as micro-reservoirs of MGLG to continuously supply lubricants. Figure 13(d) depicts the XPS curve of Ag 3d on the T3 rubbing surface under MGLG lubrication. The peaks at 368.1 and 374.2 eV belonging to metal Ag indicate that Ag did not react chemically during the friction process, which is beneficial for improving the electrical performance of the sliding electrical contacts because the pure metal generally has a better conductivity [28, 29].

A series of tribological tests show that the synergetic strategy based on LST and MGLG could effectively improve the tribological and electrical properties of Ag coatings. Figure 14 is a schematic representation of the tribological and electrical mechanisms of the non-textured and textured samples. As shown in Fig. 14(a), numerous large wear debris were generated

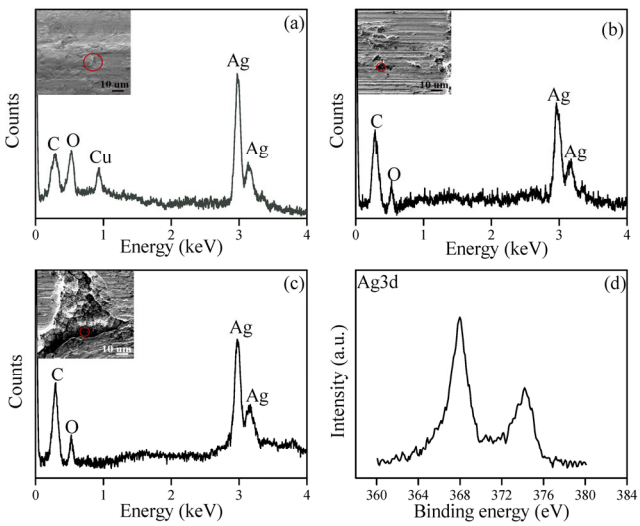

Fig. 13 EDX curves of (a) Ag under dry friction, (b) outside of the dimple (T3), and (c) in the dimple (T3) under MGLG lubrication, (d) XPS curve of Ag on the T3 rubbing surface.

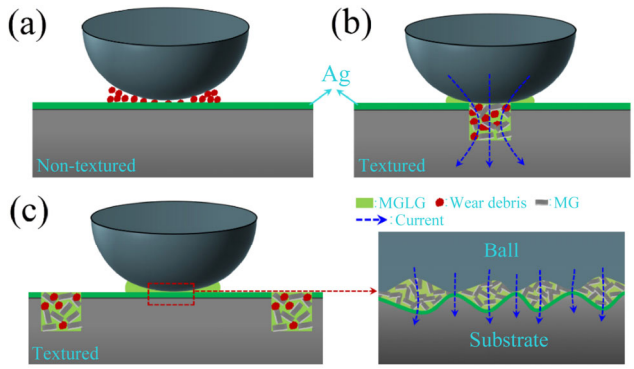

Fig. 14 Schematic representation of the tribological and electrical mechanisms of (a) non-textured coating under dry friction, (b) textured coating under MGLG lubrication, and (c) non-textured coating under MGLG lubrication.

and stacked above the wear track for the non-textured Ag coating under dry friction, resulting in severe abrasive and adhesive wear, which may be responsible for the high ECR and wear. Figures 14(b) and 14(c) illustrate the tribological and electrical mechanisms when the upper ball travels across the dimple and the smooth Ag coating under MGLG lubrication, respectively. Previous reports [17–19] confirmed that the combination of surface texture and lubricants could function as micro-hydrodynamic bearings that improve the tribological properties. Figure 14(b) shows that dimples could effectively capture the wear debris and a similar micro-hydrodynamic bearing effect could also be achieved by combining LST and MGLG to improve the tribological performances. Additionally, the wear debris of Ag and MGLG fillings in dimples can also form contact points to generate a conductive path for the flow of current. However, it should be noted that the fluctuation in the ECR may increase slightly due to the lower conductivity of the mixture filling in the dimples than that of the pure Ag. The lubrication mechanisms of MG are mainly dependent on its special structure. As shown in Fig. 14(c), MG has a two-dimensional planar structure and weak van der Waals bonds between the layers, which can readily form a shearing protective film between friction interfaces to decrease the direct asperity contact, thereby greatly enhancing the tribological properties [30, 31]. This possible lubrication mechanism could be supported by the result shown in Fig. 13(b), where the EDX spectra suggests that MG was present on the rubbing surface to form a protective film. As for the conductivity, when the upper ball travels across the smooth Ag coating under MGLG lubrication, the MGLG existing between the contact interfaces could also form conductive paths to transmit current, thereby improving the electrical performance of the sliding electrical contacts. Meanwhile, the XPS spectra of Ag (Fig. 13(d)) suggests that Ag did not react chemically under MGLG lubrication, which is beneficial for improving the electrical performance of sliding electrical contacts because pure Ag generally has a better conductivity.

4 Conclusions

In the present study, a synergetic strategy based on LST and MGLG was developed to enhance the tribological and electrical performances of Ag coatings for sliding electrical contact application. The conclusions are summarized as follows:

1) MG-doped bentone grease exhibited preferable thermal stability, anti-corrosion, and tribological properties.

2) Under MGLG lubrication, the textured Ag coatings with dimple diameters of 244 and 307 μm exhibit excellent tribological and electrical properties under the low and high current density.

3) When the Ag coating was subjected to heat treatment, the dimples on the coating could prompt thermal stress to concentrate around the edges of the dimples and dissipate, thereby preventing the decrease in the binding force between the Ag coating and the substrate and improving the tribological and electrical properties.

4) Such good tribological and electrical performances are mainly attributed to the synergetic effect of LST and MGLG. Dimples on the Ag coating could effectively capture the wear debris and function as micro-reservoirs of lubricants and micro-hydrodynamic bearings during the friction process, thereby improving the tribological and electrical properties. Meanwhile, MGLG could form a protective film and generate conductive paths to enhance the tribological and electrical properties.

Acknowledgements

This work is supported by the Natural Science Foundation of Beijing Municipality (No. 2172053)

and National Natural Science Foundation of China (No. 51575181).

Reference

[1] Grandin M, Wiklund U. Friction, wear and tribofilm formation on electrical contact materials in reciprocating sliding against silver-graphite. *Wear* **302**(1-2): 1481–1491 (2013)

[2] Deng C, Yin J, Zhang H, Xiong X, Wang P, Sun M. The tribological properties of Cf/Cu/C composites under applied electric current. *Tribol Int* **116**: 84–94 (2017)

[3] Bouchoucha A, Chekroud S, Paulmier D. Influence of the electrical sliding speed on friction and wear processes in an electrical contact copper-stainless steel. *Appl Surf Sci* **223**(4): 330–342 (2004)

[4] Grandin M, Nedfors N, Sundberg J, Jansson U, Wiklund U. Ti-Ni-C nanocomposite coatings evaluated in a sliding electrical contact application. *Surf Coat Technol* **276**: 210–218 (2015)

[5] Nedfors N, Primetzhofer D, Wang L P, Lu J, Hultman L, Jansson U. Characterization of magnetron sputtered Cr-B and Cr-B-C thin films for electrical contact applications. *Surf Coat Technol* **266**: 167–176 (2015)

[6] Bares J A, Argibay N, Dickrell P L, Bourne G R, Burris D L, Ziegert J C, Sawyer W G. In situ graphite lubrication of metallic sliding electrical contacts. *Wear* **267**(9): 1462–1469 (2009)

[7] Ren W B, Wang P, Song J, Zhai G F. Effects of current load on wear and fretting corrosion of gold-plated electrical contacts. *Tribol Int* **70**: 75–82 (2014)

[8] Trinh K E, Tsipenyuk A, Varenberg M, Rosenkranz A, Souza N, Mücklich F. Wear debris and electrical resistance in textured Sn-coated Cu contacts subjected to fretting. *Wear* **344-345**(4): 86–98 (2015)

[9] Plesca A. Thermal analysis of sliding electrical contacts with mechanical friction in steady state conditions. *Int J Therm Sci* **84**: 125–133 (2014)

[10] Wang Z Y, Xia Y Q, Liu Z L, Hu T C. Friction and wear behaviour of laser-textured surfaces under the lubrication of polyurea grease containing various additives. *Proc Inst Mech Eng Part J* **225**(3): 139–150 (2011)

[11] He D, Zheng S, Pu J, Zhang G, Hu L. Improving tribological properties of titanium alloys by combining laser surface texturing and diamond-like carbon film. *Tribol Int* **82**: 20–27 (2015)

[12] Zhang D, Zhao F, Li Y, Li P, Zeng Q, Dong G. Study on tribological properties of multi-layer surface texture on Babbitt alloys surface. *Appl Surf Sci* **390**: 540–549 (2016)

[13] Zhang K, Deng J, Xing Y, Li S, Gao H. Effect of microscale texture on cutting performance of WC/Co-based TiAlN coated tools under different lubrication conditions. *Appl Surf Sci* **326**: 107–118 (2015)

[14] Huang Z Y, Zhai H X, Li M Q, Liu X H, Zhou Y. Friction behaviors and effects on current-carrying wear characteristics of bulk TiAlC. *Tribol Trans* **57**(2): 300–307 (2014)

[15] Cao Z F, Xia Y Q. Study on the preparation and tribological properties of fly ash as lubricant additive for steel/steel pair. *Tribol Lett* **65**(3): 104 (2017)

[16] Cao Z F, Xia Y Q, Xi X. Nano-montmorillonite-doped lubricating grease exhibiting excellent insulating and tribological properties. *Friction* **5**: 219–230 (2017)

[17] Wang X, Adachi K, Otsuka K, Kato K. Optimization of the surface texture for silicon carbide sliding in water. *Appl Surf Sci* **253**(3): 1282–1286 (2006)

[18] Kovalchenko A, Ajayi O, Erdemir A, Fenske G, Etsion I. The effect of laser surface texturing on transitions in lubrication regimes during unidirectional sliding contact. *Tribol Int* **38** (3): 219–225 (2005)

[19] Segu D Z, Si G C, Choi J H, Kim S S. The effect of multi-scale laser textured surface on lubrication regime. *Appl Surf Sci* **270**: 58–63 (2013)

[20] Cao Z F, Xia Y Q, Ge X Y. Conductive capacity and tribological properties of several carbon materials in conductive greases. *Ind Lubr Tribol* **68**(5): 577–585 (2016)

[21] Huang W, Kong L, Wang X. Electrical sliding friction lubricated with ionic liquids. *Tribol Lett* **65**(1): 17 (2017)

[22] Ge X Y, Xia Y Q, Shu Z Y. Conductive and tribological properties of lithium-based ionic liquids as grease base oil. *Tribol Trans* **58**(4): 686–690 (2015)

[23] Fan X Q, Xia Y Q, Wang L P, Li W. Multilayer graphene as a lubricating additive in bentone grease. *Tribol Lett* **55**(3): 455–464 (2014)

[24] Ge X Y, Li J J, Luo R, Zhang C H, Luo J B. Macroscale superlubricity enabled by the synergy effect of graphene-oxide nanoflakes and ethanediol. *ACS Appl Mater Inter* **10**: 40863–40870 (2018)

[25] Song H, Wang B, Zhou Q, Xiao J, Jia X. Preparation and tribological properties of MoS_2 /graphene oxide composites. *Appl Surf Sci* **419**: 24–34 (2017)

[26] Cao Z F, Xia Y Q, Liu L H, Feng X. Study on the conductive and tribological properties of copper sliding electrical contacts lubricated by ionic liquids. *Tribol Int* **130**: 27–35 (2019)

[27] Chen J H, Xia Y Q, Hu Y C, Hou B Y. Tribological performance and conductive capacity of Ag coating under boundary lubrication. *Tribol Int* **110**: 161–172 (2017)

[28] Fu X. Investigation of electrical contact resistance of Ag nanoparticles as additives added to PEG 300. *Tribol Trans* **52**(2): 157–164 (2009)

[29] Ma J, Mo Y, Bai M. Effect of Ag nanoparticles additive on the tribological behavior of multialkylated cyclopentanes (MACs). *Wear* **266**(7-8): 627–631 (2009)

[30] Lin J, Wang L, Chen G. Modification of graphene platelets and their tribological properties as a lubricant additive. *Tribol Lett* **41**(1): 209–215 (2011)

[31] Zhao J, Mao J, Li Y, He Y, Luo J. Friction-induced nano-structural evolution of graphene as a lubrication additive. *Appl Surf Sci* **434**: 21–27 (2018)

Zhengfeng CAO. He received his Ph.D. degree from North China Electric Power University in 2019. After that, he is currently a lecturer at the School of Advanced Manufacturing Engineering, Chongqing University of Posts and Telecommunications. His research interests focus on tribology of mechanical and electrical equipment, and preparation and characteristics of lubricating materials.

Yanqiu XIA. He received his Ph.D. degree in mechanical engineering from Northeastern University, China, in 1999, and was selected as a professor (Hundreds Talent Program of Chinese Academy of Sciences) in 2007. He joined the School of Energy Power and Mechanical Engineer, North China Electric Power University in 2010. His current position is a professor. His research areas cover the tribology of mechanical and electrical equipment, oil monitoring, and artificial intelligence.